Pergamon

PII: S0191–8141(97)00114–4

Journal of Structural Geology, Vol. 20, No. 5, pp. 559 to 571, 1998

0191-8141/98 $19.00 + 0.00

Deformation of mylonites in Palm Canyon, California, based on xenolith geometry

HANS-RUDOLF WENK

Department of Geology and Geophysics, University of California, Berkeley, CA 94720, U.S.A.
(wenk@seismo.berkeley.edu)

(*Received* 19 *December* 1996; *accepted in revised form* 26 *November* 1997)

Abstract—An analysis of xenoliths in granodiorite and mylonites of the Peninsular Ranges batholith in southern California documents large deformation with Von Mises equivalent strains ranging from 1 to 4. From the geometry of xenoliths in mylonites it is concluded that much of the deformation occurred by flattening. If deformation had been homogeneous, the 800 m thick mylonite sequence would have extended originally over more than 10 km. Contrary to xenoliths associated with ballooning diapirs, these in Santa Rosa mylonites show much larger strains and are elongated in the lineation direction. It is proposed that the overall deformation pattern is consistent with a top to the west shear displacement, but most of the strain in the Santa Rosa mylonites was produced in flattening, during emplacement of the partially solidified batholith. The large deformation may have produced folds that have coalesced with the foliation to accommodate the strain. © 1998 Elsevier Science Ltd. All rights reserved

INTRODUCTION

Mylonites have received a lot of attention in recent years, in part sparked by a Penrose Conference (Tullis *et al.*, 1982) with a field trip to mylonites in the Peninsular Ranges of southern California. Since then the Santa Rosa mylonite zone south of Palm Springs has become a classical site to study highly deformed rocks, both in the field and in the laboratory.

Simpson and Schmid (1983) and Simpson (1984) described excellent examples of *S–C* microstructures with consistent asymmetric augen structures and pressure shadows in this region that are clear signs of shear deformation. This supported earlier conclusions based on field studies (Sharp, 1967, 1979), introducing mylonites as part of a "Zone of Shear" as it is known on the California geological map (Rogers, 1965). These highly deformed granitic rocks and marbles have provided much suitable material to investigate microscopic deformation mechanisms (e.g. Goodwin and Wenk, 1995) and the development of crystallographic preferred orientation (e.g. O'Brien *et al.*, 1987; Wenk and Pannetier, 1990). A lot of information was accumulated about ductile deformation at conditions of amphibolite facies metamorphism of these rocks. While attention focused on the extreme degree of deformation and the large regional extent of highly deformed rocks, the question of total strain was never explored. Furthermore it has not been established how much simple shear has contributed to the overall deformation of these granitic mylonites. These two topics are the subject of the present study: What is the finite strain in this large mylonite zone, over 1 km wide and extending over more than 100 km? The detailed observations refer to rocks in the Palm Canyon region south of Palm Springs, but conclusions are likely to apply to a larger portion of the mylonite zone, as well as to many mylonitic rocks which display similar microstructures.

The aim is to evaluate strain from a statistical investigation of the shape of xenoliths (also known as enclaves, e.g. Didier and Barbarin, 1991) in highly deformed granitic rocks. A three-dimensional study is possible due to excellent outcrops in the deeply eroded canyons. The data were collected over several years during field trips by the author and students, and should represent an unbiased collection.

GEOLOGICAL BACKGROUND

Figure 1 displays a simplified geological map, and Fig. 2 a cross section of the area of interest. On the eastern edge of the Peninsular Ranges batholith, highly deformed rocks occur in a more or less continuous zone between Palm Springs (where the zone is truncated by the San Andreas fault), and Clark Valley (northeast of Borrego Springs) (where it is truncated by the San Jacinto fault) and may, after offset, continue as the Borrego Springs mylonite zone (Simpson, 1984). On Fig. 1 a few topographic reference points are indicated for orientation, as are sampling localities. Some local topographic names, which are not indicated on the map, are used in the text to help those readers who may wish to visit some of the localities. These names are readily available on U.S. Geological Survey topographic 7.5-minute quandrangles Palm View Peak, Rancho Mirage, Butterfly Peak, Toro Peak and Martinez Mtn.

Starting in the west and at the geologically lowest level (Fig. 2), the relatively undeformed eastern Peninsular Ranges batholith consists of several distinct

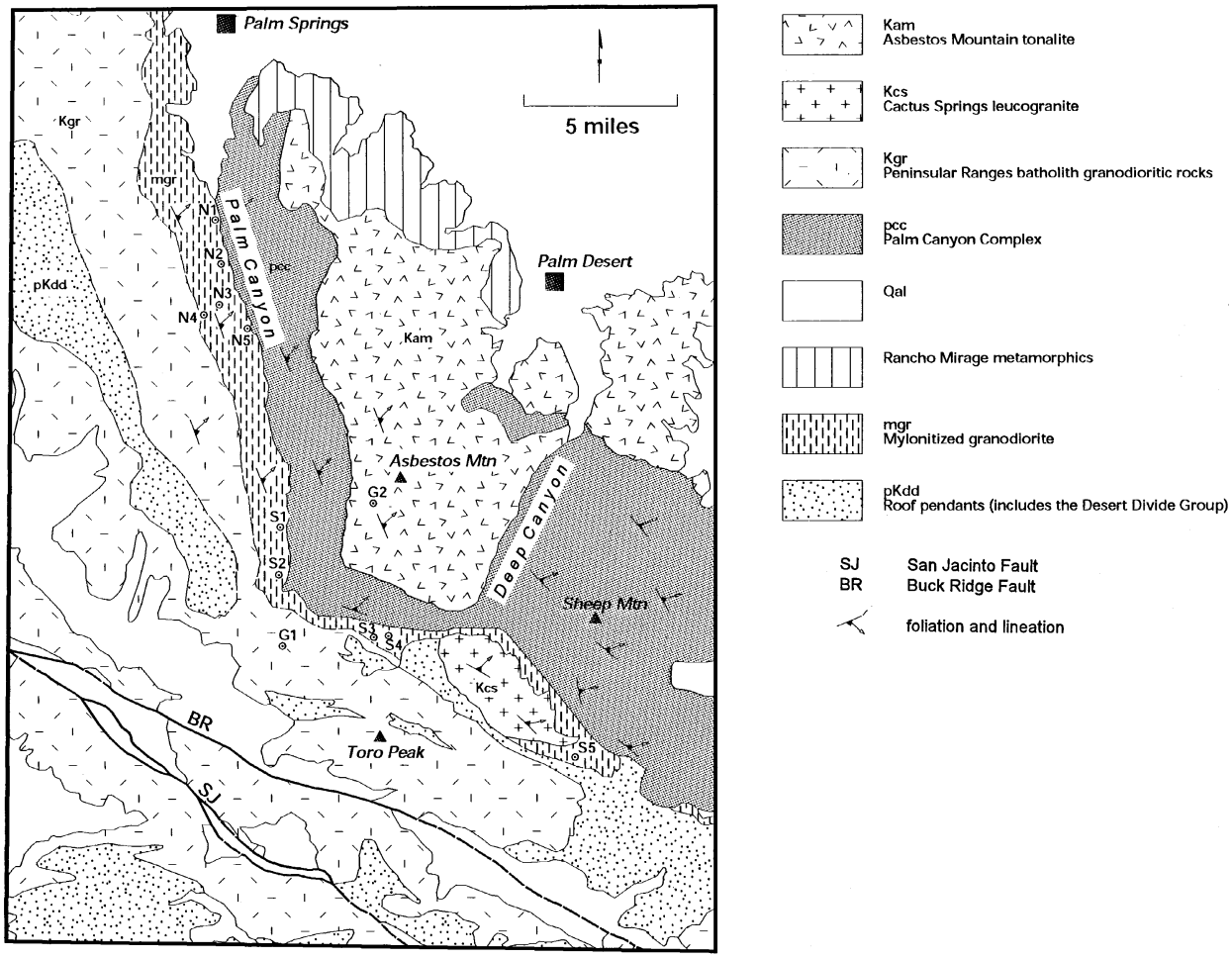

Fig. 1. Generalized geological map of Palm Canyon and adjacent areas in southern California (modified from Erskine and Wenk, 1985). Some lineations and foliations are indicated. Also shown are sampling localities (compare with Table 1).

intrusions, all of granodioritic composition (e.g. Ague and Brimhall, 1988) and Cretaceous age (97 Ma U–Pb age of zircons for the San Jacinto Mtn. Pluton, Hill and Silver, 1980). These batholitic rocks are in contact with roof pendants in the western part. To the east (western slope of Palm Canyon) the batholith is overlain by a 700–900 m thick sequence of mylonites of similar composition to the protolith and a similar igneous age (97 Ma U–Pb, B. Nelson and L. Ratschbacher, unpublished). These strongly foliated rocks are distinct in the field (Fig. 3).

During mylonitization a very regular E-plunging lineation and an E-dipping foliation developed, microscopically expressed in preferred orientation of biotite and quartz (Wenk and Pannetier, 1990) and formed during dislocation creep and dynamic recrystallization, with grainsize reduction of quartz and mica (Goodwin and Wenk, 1995). The degree of deformation is variable: an undeformed protolith with moderate deformation features, such as undulatory extinction in quartz, transforms rather abruptly into mylonites, and locally into ultramylonites and phyllonites. The latter two are extremely fine grained rocks, resembling flint and slate, but with the same overall chemical and mineralogical composition as the protolith (O'Brien *et al.*, 1987). The relatively sharp transition from protolith to mylonite can be mapped in the field and is shown on the map (Fig. 1). Equally, ultramylonites and phyllonites form well-defined zones, ranging from 2 cm in thickness to 20 m. They are most common in upper Palm Canyon (near highway 74, between localities S2 and S3) and the southern extension where the mylonite zone is narrowest (between localities S4 and S5).

The granodioritic mylonites are overlain by metamorphic rocks of the Palm Canyon Formation. These are in ordinary igneous contact with the batholitic rocks in the northern part (near locality N1 at Hermit's Bench at the bottom of Palm Canyon, south of Palm Springs). In most places the contact is not exposed, in some places it appears as a fault with substantial hydrothermal alteration, and in some areas the Palm Canyon formation. is separated from the granodioritic mylonites by an intruded porphyritic tonalite (Fig. 2). The metamorphic rocks have various lithologies: pelitic and leucocratic gneisses (with granulitic texture), migmatites, amphibolites (characteristically with oxyhornblende), pyroxenites, calcsilicates (with

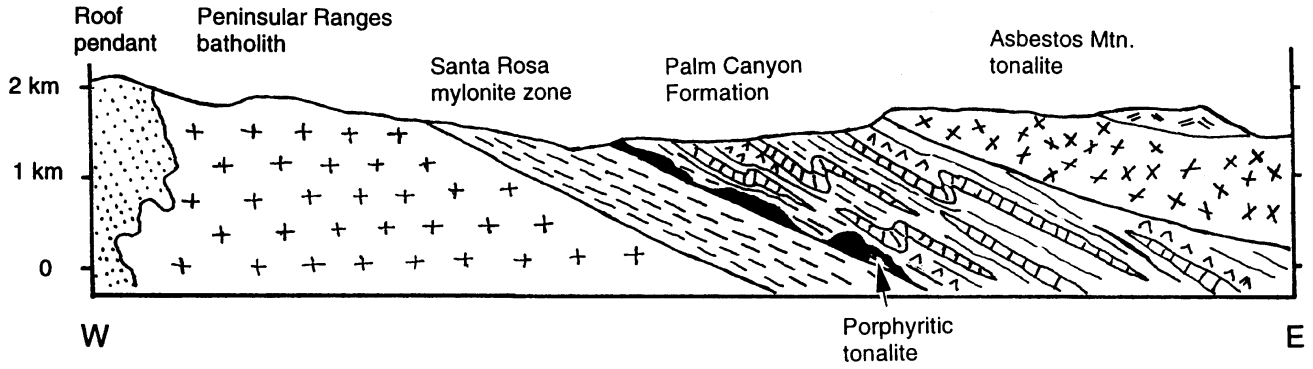

Fig. 2. E–W cross section through the Santa Rosa mylonite zone in central Palm Canyon. No vertical exaggeration.

forsterite, diopside and scapolite) and marbles. The metamorphic grade is upper amphibolite facies as established by index minerals such as sillimanite and cordierite in pelitic schists, forsterite in marbles, and orthopyroxene and spinel in amphibolites.

Deformation of the Palm Canyon formation is very heterogeneous. For example carbonate rocks may exist as coarse marble or as fine-grained ultramylonites. These calcite ultramylonites could be mistaken in the field for unmetamorphosed limestones, were it not for calcsilicate clasts of forsterite and diopside, documenting a metamorphic origin. As in the underlying mylonites, shear indicators such as asymmetric tails around porphyroclasts on a microscopic scale, and shear bands on a macroscopic scale, are consistent with a top-to-the-west movement. Lineations in the Palm Canyon formation are parallel to those in the underlying mylonites, suggesting that they were deformed at the same time. Migmatites in the Palm Canyon formation and its southern extension (towards Sheep and Martinez Mountains) are often mylonitic. A U–Pb age of zircons in migmatites of 110 Ma (Nelson and Ratschbacher, unpublished) indicates that the metamorphism is of a similar age as the batholitic intrusions (inheriting some old components), rather than an older event. Occasionally folding is observed and the fold axes are always parallel to the lineation. In the upper (and south eastern) part of the Palm Canyon formation deformation of migmatites is more brittle, with an extensive zone of pseudotachylites (Wenk and Pearson, in preparation). The cataclastic rocks are best exposed in Deep Canyon and southwest of Palm Desert.

The Palm Canyon formation and associated rocks are overlain by the Asbestos Mountain granodiorite of tonalitic composition (U–Pb age of 87 Ma, Nelson and Ratschbacher, unpublished). The structure of Asbestos Mountain tonalite is reminiscent of a gently

Fig. 3. View from the western slope of Palm Canyon towards Santa Rosa Mountain in the background. In the foreground are strongly foliated mylonites, on the eastern slope of Palm Canyon (left) are metamorphic rocks of the Palm Canyon Formation.

Fig. 4. More or less equiaxed xenoliths with random orientation in undeformed plutonic rocks at Spring Crest (locality G1). Hammer handle is 50 cm.

inclined sheet with roots north and south of Palm Desert. The igneous contact with the underlying Palm Canyon formation is characterized by skarns. Asbestos Mountain tonalite is undeformed with igneous microstructures.

Goodwin and Renne (1991) used K–Ar cooling ages of cataclastic biotite to place the onset of mylonitic deformation at 89 Ma. Cecil (1990) determined $^{40}Ar/^{39}Ar$ ages of biotite and hornblende by thermal release to find that the cooling path of Palm Canyon metamorphic rocks is intermediate between that of Peninsular Ranges granodiorite and Asbestos Mtn. tonalite. The youngest ages of 64 Ma, post-dating deformation, are fission track dates of zircon, sphene and apatite (Dokka, 1984). From the geochronological studies it is clear that the high-grade metamorphism is related to the Cenozoic plutonic activity and that deformation started with the emplacement of the batholithic rocks and extended into the cooling period. Initially deformation was ductile and later became increasingly brittle, as evidenced by ductile–brittle faults, cataclasites and pseudotachylites. The exact timing and duration of the mylonitic deformation is still unknown.

STRAIN ANALYSIS

The Peninsular Ranges granodioritic rocks are chemically and structurally fairly homogeneous; however, they do represent different intrusions. The main constituent minerals are plagioclase, quartz, biotite, orthoclase and some hornblende. Locally they contain swarms of enclaves that are of similar composition, although enriched in biotite and hornblende. Mechanical properties of inclusions and matrix are similar and, based on aspect ratios of grains such as quartz, deformation appears to be uniform. As will be shown, these xenoliths are (statistically) more or less equiaxed in undeformed granodiorite (Fig. 4) and attain a highly ellipsoidal shape in mylonites (Fig. 5). By measuring the shape of xenoliths one can get information about the total deformation and and put some constraints on the deformation history. This method has been used to investigate deformation during pluton emplacement (e.g. Hutton, 1982; Ramsay, 1989; Tobisch *et al.*, 1993). Almost all these analyses reported two-dimensional data, assuming that xenoliths are axially symmetric (pancake shape).

During homogeneous deformation, a sphere changes its shape into an ellipsoid. Since there is no significant porosity in these rocks, it is safe to assume that the volume is preserved. Assuming that the original shape is a sphere, the shape (axes lengths) and orientation of a strain ellipsoid can be obtained by an infinite number of different deformation paths. However, if one assumes uniform deformation, the total strain and some aspects of the strain history can be interpreted from the shape.

Structural geologists have refined the methodology to estimate strain from observations on enclaves in igneous rocks. Considerable effort was invested in determining the relationship between the original shape distribution of inclusions, and that after deformation (e.g. Hutton, 1982). The R_f/ϕ method proposed by Ramsay (1967, pp. 202–211) and advanced by Lisle (1985) is an elegant approach for moderately deformed rocks. The deviation from ideally ellipsoidal shape has an influence on the final shape, as demonstrated by

Fig. 5. Strongly deformed xenoliths in mylonite at Dry Wash (locality N2).

Treagus *et al.* (1996) with a finite element analysis. For the cases described here both these refinements are not considered very relevant. At the high deformations in the mylonites of Palm Canyon all major axes of inclusions have become subparallel to mesoscopic fabric coordinates (long axis parallel to the lineation, and short axis normal to the foliation). Even though the highly deformed inclusions may not be ideal ellipsoids, the determination of axis lengths in the field, and a statistical analysis of aspect ratio distributions, seems most appropriate to obtain a strain estimate in these rocks.

As a measure of the total strain Von Mises equivalent strain ε_{eq} for coaxial deformation is used. This is a convenient measure, used in engineering, to compare experimental stress–strain curves for different strain histories and is universally applied in polycrystal plasticity simulations

$$\varepsilon_{eq} = \sqrt{[2/3(\varepsilon_1^2 + \varepsilon_2^2 + \varepsilon_3^2)]} \quad (1)$$

where $\varepsilon_1 = \ln a/d$, $\varepsilon_2 = \ln b/d$ and $\varepsilon_3 = \ln c/d$, with d the diameter of the original sphere and a, b, c the axial lengths of the ellipsoid. The diameter of the sphere can be obtained from the ellipsoid axes, assuming that the volume remains constant

$$d = (abc)^{1/3}. \quad (2)$$

Figure 6 shows, for flattening ($\varepsilon_1 = \varepsilon_2$) and plane strain ($\varepsilon_2 = 0$), a/c ellipsoid sections for equivalent strains of 0, 0.5, 1 and 2 and provides some indication of the degree of deformation. As will be demonstrated below, most xenoliths in Santa Rosa mylonites have equivalent strains > 2.

For analyzing simple strain histories a Flinn diagram, representing ratios of axes lengths, is useful (Fig. 7) (Flinn, 1962 and discussion in Ramsay and Huber, 1983, p. 172). Since ratios are used, this representation corrects for absolute size. Assuming that $a \geq b \geq c$, a sphere plots at coordinates 1:1. If a sphere deforms in constriction to a prolate shape ($b = c$), it plots along the ordinate ($b/c = 1$) with increasing values for increasing deformation. In flattening ($a = b$) data plot along the abscissa ($a/b = 1$). A special case is the diagonal in a Flinn diagram with $a/b = b/c$. This represents deformation in plane strain. Plane strain is the geometry during simple folding or shearing and is thought to be geologically most important. The distance of a data point from the origin (1:1) is indicative of the overall deformation. In the literature often logarithmic ratios are used, enforcing the condition $a \geq b \geq c$. In this application direct ratios are more appropriate since a, b and c are defined with respect to mesoscopic fabric coordinates and ratios may be smal-

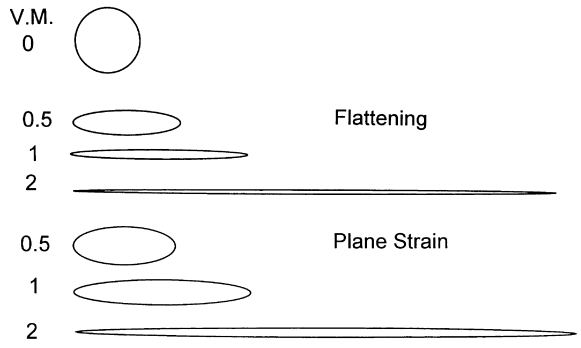

Fig. 6. Two-dimensional representation of the deformation of a sphere into an ellipsoid for Von Mises equivalent strains of 0.5, 1 and 2, shown as a–c ellipse sections for axial compression (flattening) (top) compared to plane strain (bottom).

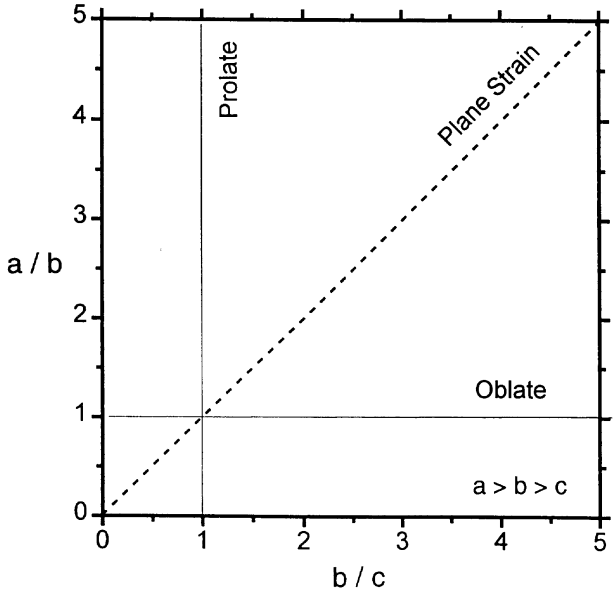

Fig. 7. Schematic Flinn diagram illustrating regions of prolate strain, plane strain and oblate (flattening) strain as function of aspect ratios. In the case of xenoliths in this study a is parallel to the lineation and c normal to the foliation. The condition $a > b > c$ does not apply to all individual xenolith measurements.

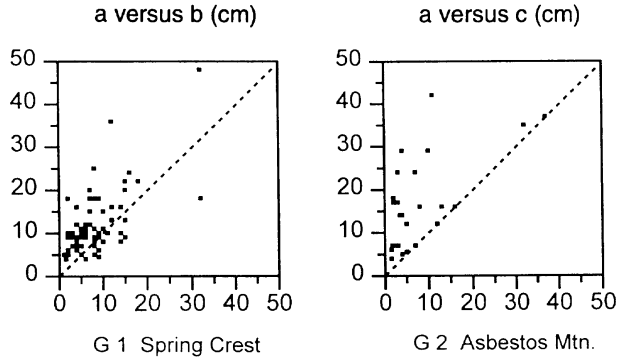

Fig. 8. Dimensions of xenoliths observed at two localities of undeformed plutonic rocks.

ler than 1 for a few cases where the original shapes are not spherical.

If all three principal xenolith axes can be measured in the field, the analysis is straightforward. In many cases one is restricted to two-dimensional outcrops and can only measure two axes. In this case average values for a/b and b/c ratios can be obtained, measured on two faces, and the averages represented on the Flinn diagram. Even for homogeneous deformation one expects some scatter for an individual outcrop because initial xenoliths are not ideal spheres. It is therefore necessary to sample a statistically representative number. A minimum of 15 xenoliths (five with all axes measured) was collected at each locality. The raw measurements are shown in Figs 8–11. Average ratios were obtained by least squares (Table 1 and Fig. 12). The influence of the initial xenolith shape is more important for weak than for strong deformation.

Dimensions were measured at 12 locations, indicated in Fig. 1. Two of those are xenolith swarms in undeformed protolith, the rest are swarms in granite mylonite. In the representation the data are divided into undeformed protolith (G1 and G2), the northern zone that is representative of the large, impressive N–S trending mylonites in Palm Canyon (N1–N5), and the southern zone (Upper Palm Canyon and extending south of highway 74) that is associated with a bend in the contact and phyllonites (S1–S5). In this southern zone, deformation is locally extreme and less homogeneous than in the northern zone.

RESULTS

Overall dimensions of 567 xenoliths were analyzed in mylonites. In 151 of those all three axes could be measured. Table 1 summarizes these data. Original xenolith sizes show some spread. The largest that was measured has a diameter of 40 cm, the smallest of 3 cm, but most range between 5 and 15 cm and the average diameter of 151 xenoliths for which all three axes could be measured is 10.3 cm. There is no significant variation in sizes between localities, and no correlation of size with deformation.

At most localities the deformation is intense, with equivalent strains clustering between 1.5 and 3 and the largest strain of 4.5. Strains in the southern part are lower than in the north. A section from xenoliths near the undeformed protolith at Bull's Eye (N5: 1.1) to Indian Portrero (N4: 1.6) and to mylonites in Palm Canyon (N3: 3.3) documents an increase in deformation approaching the contact with the Palm Canyon Formation Data for xenolith dimensions are represented in Figs 8–12.

Protolith

Xenoliths in the protolith were measured at two localities. These xenoliths are generally angular and deviate from an ellipsoidal shape. Therefore it is difficult to assign principal axes. In a road cut at Spring Crest (G1, Fig. 4) simply horizontal and vertical dimensions of xenoliths were measured on a vertical face. There is a wide distribution of sizes and also a distribution in shapes (Fig. 8). Overall there is a slight tendency for the horizontal direction to be longer (5:4).

A second outcrop is along Palm Canyon Drive near Asbestos Mtn. The outcrop surface is irregular. In this case large (a) and small axes (b) of individual xenoliths were measured, irrespective of their orientation. The distribution is similar as before, except that, naturally, $a > b$.

There are many other locations where qualitatively similar patterns are observed. Good outcrops exist along the Mt. San Jacinto trail. In general, xenolith

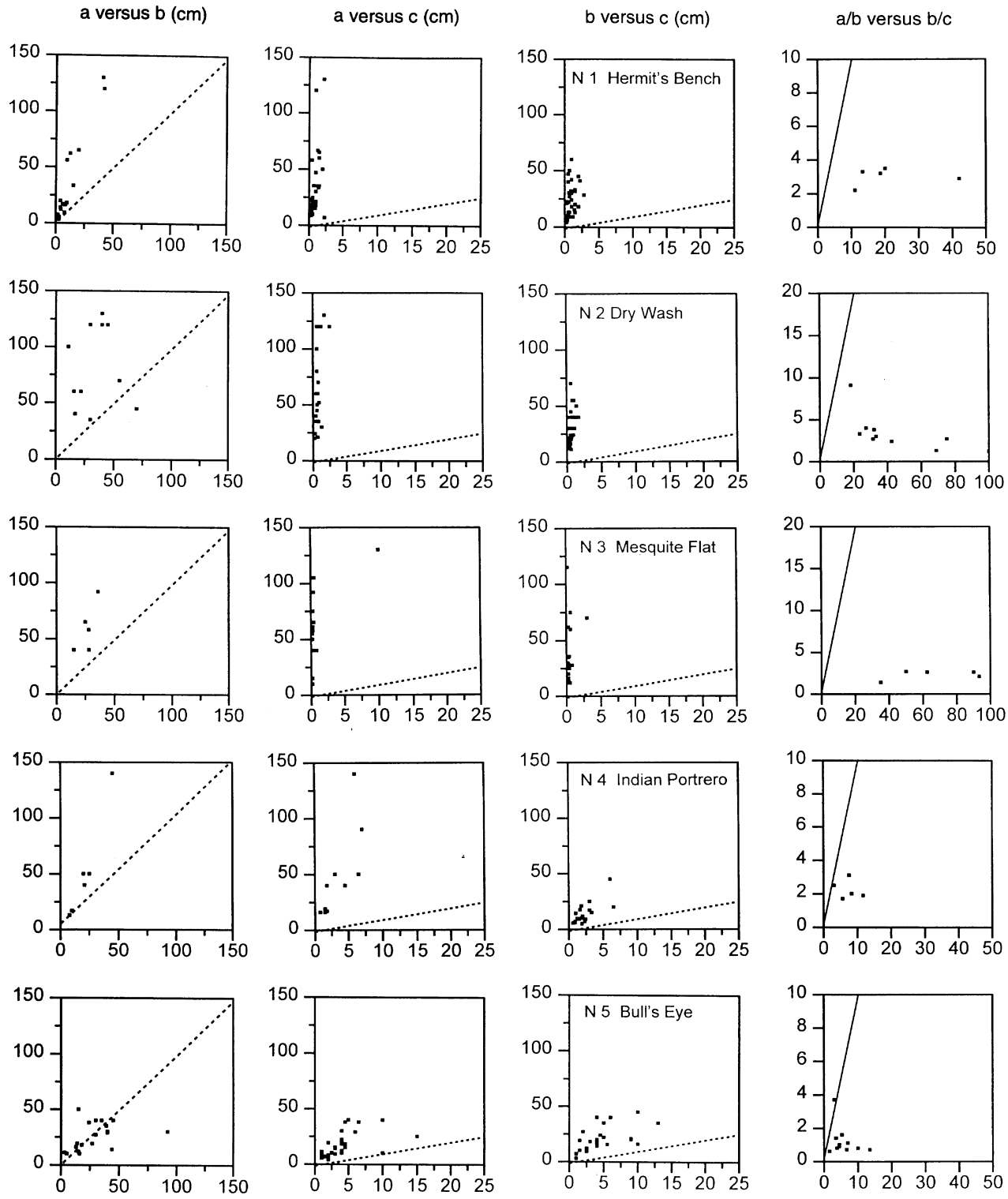

Fig. 9. Dimensions (axis lengths and ratios) of xenoliths at five localities of the northern study area. Dashed diagonal lines indicate the $a = b$, $a = c$ or $b = c$ loci, the solid diagonal line the $a/b = b/c$ locus (plane strain). The first three columns contain data for all xenoliths which were measured, the Flinn diagrams in the last column only have data for xenoliths where all three dimensions could be measured.

swarms in the protolith display a distribution in aspect ratios ranging from 1:1 to 1:4 but are irregularly oriented so that the average is close to a sphere. Individual xenoliths deviate and do not have an ideal ellipsoidal shape.

Northern area

In the mylonitic granites with clearly developed lineation and foliation, a is defined as the length parallel to the lineation and c that normal to the foliation.

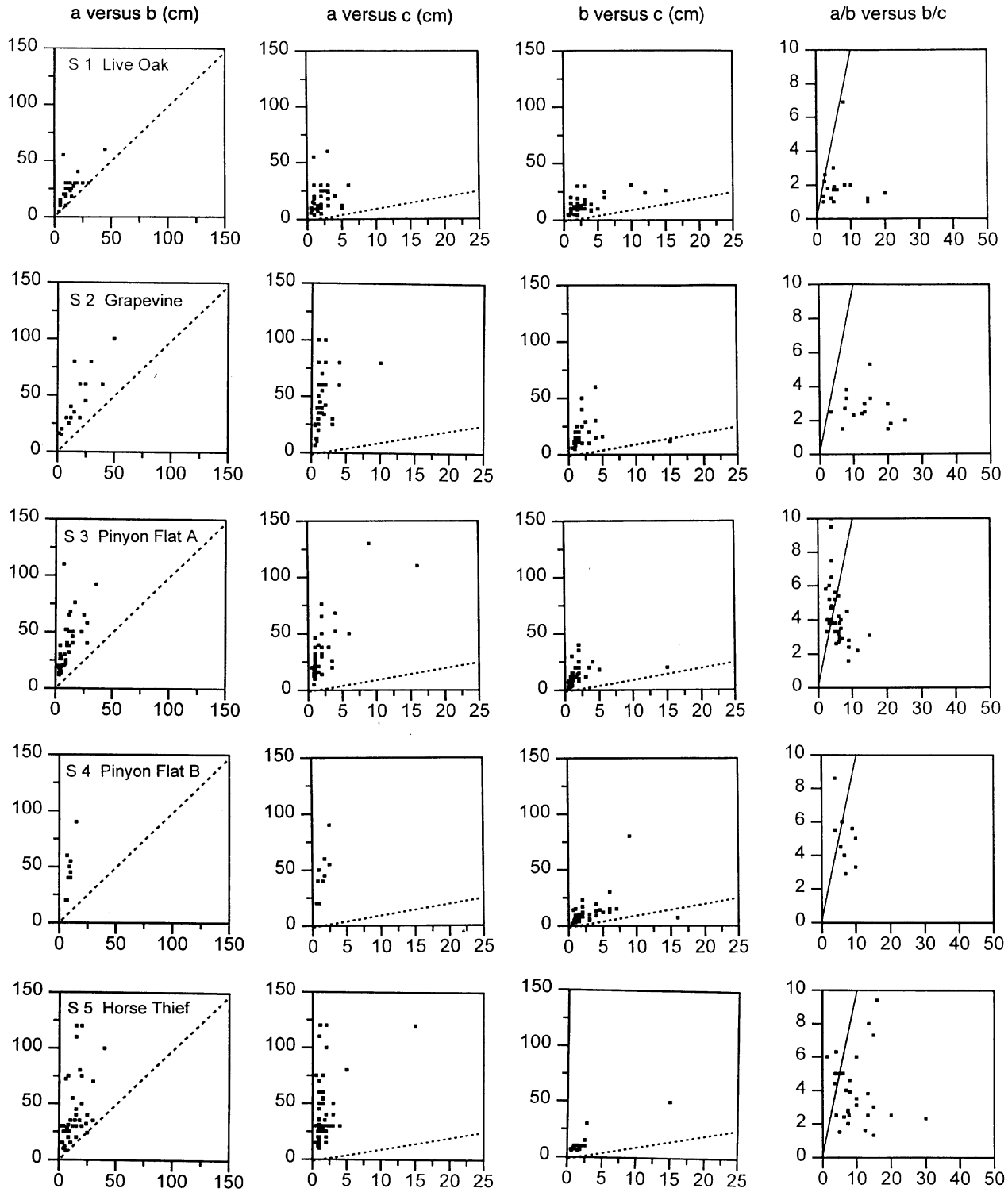

Fig. 10. Dimensions of xenoliths at five localities of the southern study area. See caption to Fig. 9.

Therefore the condition $a > b > c$ does not necessarily hold for individual xenoliths. In the northern area, a is generally larger than b and, except for N5; a and b are always much larger than c (Table 1 and Fig. 9). This is amplified in the Flinn diagram for xenoliths on which all three dimensions could be determined: all xenoliths plot in the field of flattening (the line of plane strain is indicated). Particularly for N1–N3 which are representative of the extensive Palm Canyon suite of mylonites, deformation is very large and the strain is almost pure flattening. Apart from one xenolith in N5, a/b never exceeds b/c. Outcrop N2 at the end of a dry wash in Palm Canyon is a classical locality that documents the extreme deformation on three-dimensional polished outcrops (Fig. 5). It also illustrates the coincidence of the flattened xenoliths with the plane of foliation. The

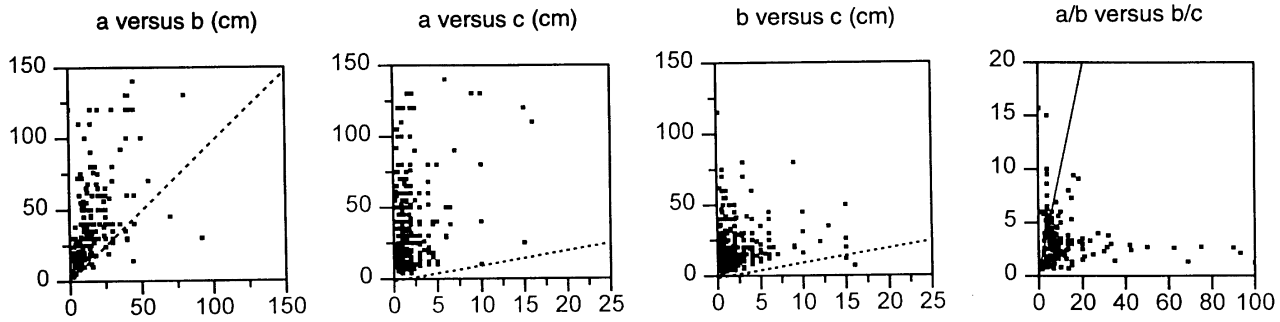

Fig. 11. Cumulative diagram illustrating the dimensions of all measured xenoliths.

oblate xenoliths are slightly elongated along the lineation ($a > b$), except for the Bull's Eye locality near the contact with nearly circular cross sections ($a = b$). Outcrops N4 and N5 are near the contact with the undeformed protolith and the strain is lower, yet the pattern very similar. Judging from the xenolith shapes along this traverse, strain increases from the protolith towards the contact with the Palm Canyon Fm. (N5, N4 and N3).

Southern area

In the southern area, close to the structural bend, the pattern is a bit different (Fig.10). There is a larger difference between a and b (always $a > b$, i.e. all xenoliths are elongated parallel to the lineation) and $a,b > c$, except for two odd cases, but the difference is smaller than in the northern area. The average strain is lower than for localities N1–N3 but, as the Flinn diagrams illustrate, for S1 and S2 (in upper Palm Canyon) deformation is still by flattening. For the southern localities S3–S5 deformation is closer to plane strain, particularly for more highly deformed xenoliths. All of these localities are within 100 m of the contact with undeformed protolith. In this southern area the mylonite zone is narrow and mylonites grade rapidly into phyllonites. In the phyllonites xenoliths could no longer be identified.

Two additional figures summarize the results. One gives the distributions for all 567 xenoliths (151 for the Flinn diagram), irrespective of location (Fig. 11), and illustrates a dominant tendency for flattening. This diagram is somewhat biased because more xenoliths were measured in the southern area (Table 1). Figure 12 summarizes a/b and b/c averages for each locality, based on all xenoliths, not just those where all three axes could be determined. By least squares the mean axis ratios from all axis measurements in a particular section were determined and these averages are then represented in a Flinn diagram. Corresponding numerical data are also listed in Table 1. The picture established in Figs 9–11 is confirmed: typical mylonites (N1–N3) are strongly deformed in flattening. Near the contact with the undeformed protolith (N4–N5 and S1–S3) strains are less extreme, and in the southern area deformation is closer to plane strain (S3–S5).

DISCUSSION

The investigation of xenolith shapes in Santa Rosa mylonites has revealed interesting patterns. It is obvious that an analysis requires a statistically representative distribution. Individual xenoliths had deviations from spherical shape and arbitrary orientations before deformation and both features affect the final geometry. However, as long as a representative distribution is considered, individual shapes are irrelevant if there is no initial preferred orientation. Also, for large deformations, even an initial igneous alignment of

Table 1. Statistical data. Diameter of original sphere and equivalent strain (with standard deviations) are for 151 deformed xenoliths for which all three axes could be measured (3D). Average axis ratios are for all 567 xenoliths (2D), obtained by least squares. Undeformed xenoliths (G) are added for completeness

Locality	Number (3D)	Number (2D)	Diameter (cm)	Equiv. strain (ε_{eq})	a/b	b/c	a/b:b/c
G1 Spring Crest	6	68					
G2 Asbestos Mtn.	0	26					
N1 Hermit's Bench	5	48	12.7 (7.8)	2.4 (0.4)	3.1	30.3	9.8
N2 Dry Wash	11	93	12.3 (4.8)	2.9 (0.2)	2.8	50.0	17.9
N3 Mesquite Flat	6	33	10.0 (4.0)	3.3 (0.6)	2.1	90.9	43.3
N4 Indian Portrero	5	25	17.2 (10)	1.6 (0.3)	2.8	6.6	2.4
N5 Bull's Eye	11	53	13.9 (6.3)	1.1 (0.3)	1.0	4.7	4.7
S1 Live Oak	18	72	8.1 (3.3)	1.4 (0.5)	1.9	4.4	2.3
S2 Grapevine	14	62	14.4 (7.7)	2.1 (0.4)	2.9	7.5	2.6
S3 Pinyon Flat A	41	68	8.3 (7.4)	1.8 (0.2)	3.4	5.8	1.7
S4 Pinyon Flat B	9	15	8.5 (3.3)	2.0 (0.2)	5.6	4.4	0.8
S5 Horse Thief	31	98	9.6 (6.3)	2.0 (0.4)	4.0	8.7	2.2

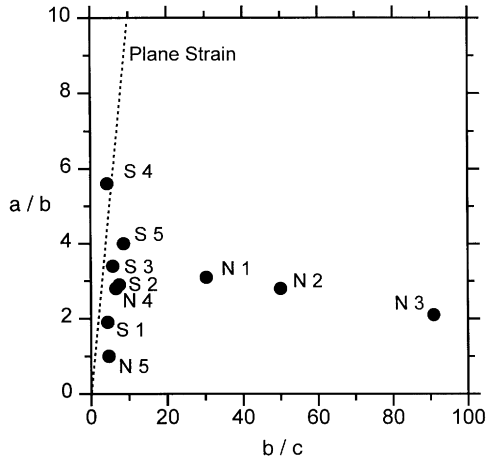

Fig. 12. Flinn diagram illustrating averages for all xenoliths studied at the 10 localities. For locations see Fig. 1 and for statistical information see Table 1.

xenoliths (that was not observed in the undeformed Peninsular ranges batholith) would not affect the pattern in deformed xenoliths significantly. All their major axes are more or less parallel with the mesoscopic fabric coordinates. The fact that in the vast majority of cases $a,b > c$ indicates that the influence of the original igneous xenolith shape is minor and that the regular pattern of xenolith geometry is mainly due to deformation in solid state.

From petrographic evidence and microstructures in the mylonites it appears that deformation of matrix and xenoliths was ductile and fairly homogeneous. Of the mineral components, feldspars and occasional hornblende are mainly porphyroclastic and are present as rigid inclusions, quartz grains are either flattened or dynamically recrystallized with a regular, often asymmetric, flow pattern around the inclusions. If anything, the more melanocratic xenoliths, with a higher content in hornblende, may be slightly stiffer and strain determined from the xenolith geometry could be underestimated.

O'Brien *et al.* (1987) studied the preferred orientation of biotite in mylonites and phyllonites of the same zone and determined March strains. Their results are recalculated (Table 2) and represented in a Flinn diagram (Fig. 13). Equivalent strains from phyllosilicate textures are much lower than those from xenolith shapes. This is not surprising because at large strains phyllosilicates do not satisfy the March condition of behaving like passive markers in a viscous medium, as has been documented experimentally (Tullis, 1976; Sintubin *et al.* 1995). Deviations from the March model are particularly severe for heterogeneous polyphase materials such as granodiorite with fairly rigid inclusions of plagioclase and hornblende. Furthermore, phyllosilicates in these mylonites are generally recrystallized with significant grain size reduction (Goodwin and Wenk, 1995). The results from this study demonstrate that the March model cannot be used quantitatively to predict strain in these mylonites. However, this independent strain evaluation from phyllosilicate preferred orientation also suggests a flattening geometry, with most a/b ratios near 1.

The geometry of xenoliths has been mainly used to investigate processes during pluton emplacement and magma solidification. As early as 1937, Balk estimated strains based on shape ratios of enclaves. These methods were refined and applied to a large number of plutons, including the Sierra Nevada in California (Tobisch *et al.*, 1993; Guglielmo, 1993), the Chindamora batholith in Zimbabwe (Ramsay, 1981, 1989) and the Ardara pluton in Ireland (Holder, 1981). In all of these cases the intrusions are post-tectonic and the enclave geometry reflects the strain history during diapiric emplacement of the batholiths. Strain patterns are usually concentric with the individual pluton and high deformation is sometimes associated with a particular intrusion stage, in the case of the Chindamora pluton to the tonalitic phase. Narrow zones of intense xenolith deformation are often observed at the contact between two intrusions as shown for the Mt. Givens pluton (Tobisch *et al.,* 1993), or the contact between El Capitan and Half Dome granodiorites in Yosemite (Bateman and Wahrhaftig, 1966). Based on such xenolith observations, the geometry of pluton emplacement has been described as post-tectonic 'ballooning' (Ramsay, 1989). Paterson (1988) and Paterson and Fowler (1993) proposed a more complicated process that combines pre-

Table 2. Strain estimates based on preferred orientations in phyllosilicates (O'Brien *et al.*, 1987)

Sample	Equiv. strain (ε_{eq})	a/b	b/c	$a/b{:}b/c$
A1	0.43	1.1	1.9	1.7
B6	0.98	1.4	3.7	2.6
B8	1.07	1.3	4.2	3.2
B9	0.93	1.4	3.4	2.4
B9*	0.75	1.0	3.0	3.0
B10	0.99	1.4	3.7	2.6
C3	0.93	1.3	3.4	2.6
C5	0.93	1.3	3.5	2.7
C5*	0.87	1.1	3.5	3.2
D1	0.88	1.3	3.3	2.5

*Indicates a second sample from the same location.

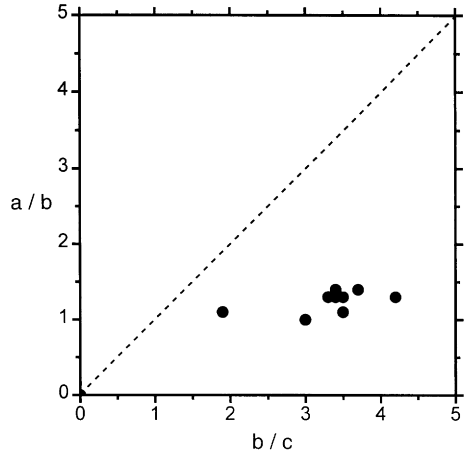

Fig. 13. Flinn diagram derived from March strains, obtained from biotite preferred orientations in phyllonites (O'Brien *et al.*, 1987) (cf. Table 2).

tectonic diapiric intrusion, short and long distance material transfer and post-tectonic ballooning.

In some of these examples cited there is moderate mechanical interaction between pluton and surrounding wallrock, but deformation of the pluton is not related to a large regional ductile deformation, as in the case for the Santa Rosa mylonite zone described in this paper. Here xenolith deformation is strictly confined to the eastern contact of the batholith with the Palm Canyon Fm. The mylonitic foliation is a regular planar structure that extends over more than 100 km, cutting across individual intrusions, and consistent with the overlying metamorphic rocks of the Palm Canyon Fm. (Fig. 1). The zone of deformation does not have shape of a diapir necessary to accommodate deformation by a ballooning mechanism during emplacement. Also, the deformed rocks have a mylonitic microstructure, contrary to many of the plutons, e.g. in the Sierra Nevada, where the microstructure even of strongly flattened xenoliths is granular or granophyric (e.g. Guglielmo, 1993). In this respect, the Santa Rosa mylonites resemble the Tertiary Bergell granite in the Alps which has been in large portions penetratively deformed with its wallrock, and also displays mylonitic microstructures with flattened and dynamically recrystallized quartz, wrapping around feldspar clasts (Wenk, 1973).

The present study documents that xenoliths provide a means by which to estimate overall deformation and can be used to obtain information about the deformation history of granite mylonites. The results for lower and central Palm Canyon (N1–N3) that are representative of a massive mylonite sequence, illustrate very large deformations ($\varepsilon_{eq} = 2$–4) with a/c ratios in the vicinity of 100. Assuming pure flattening, this implies that for homogeneous deformation the 800 m thick sequence of mylonites in Palm Canyon originally had a thickness of over 10 km. These strains are higher than those in the pluton studies referred to above.

It has been startling to find consistently highly flattened xenoliths with a large deviation from plane strain. In this respect the xenoliths resemble those described in many diapiric plutons. As far as the Santa Rosa mylonite zone is concerned much discussion has centered on the importance of simple shear and pure shear. Simpson (1984) proposed a non-coaxial thrust based on asymmetric microstructures, and Erskine and Wenk (1985) inferred coaxial deformation based on highly symmetric fabric patterns of quartz and calcite in rocks of the associated Palm Canyon Formation. These patterns of xenolith shapes are not compatible with plane strain deformations of pure shear or simple shear.

The tendency for large strains and flattening is most pronounced for locations N1–N5 and S1–S2. The southern localities display patterns of lower strain and the xenolith shape is closer to plane strain: S3–S4 are near the structural bend with the contact parallel to the lineation due to the emplacement (and offset) of the Santa Rosa Mtn. granodiorite; S5 is far south in the vicinity of Cactus Springs leucogranite. In this discussion flattening has been emphasized as deformation geometry, inconsistent with shearing and similar to xenoliths observed in diapirs. But contrary to those diapirs, all xenoliths in the Santa Rosa mylonite zone are elongated in the lineation direction ($a > b$), except for one locality (N5 Bull's Eye). The well-developed lineation has been interpreted as a stretching lineation (Simpson, 1984).

How can an extensive mylonite sequence accommodate a large flattening strain? The material has to flow radially in all directions, which is in apparent contradiction with the overwhelming evidence for a preferred NE–SW directionality and a pervasive lineation. Part of the deformation may be attributed to pluton emplacement along Palm Canyon with some geometric constraints. It has been mentioned above that folding is observed, mainly in the vicinity of the contact with the Palm Canyon Fm., where lithologic heterogeneity provides marker horizons, and within metamorphic rocks of the Palm Canyon Fm. Wherever folds are recognized, fold axes are parallel to the lineation. In the strongly deformed mylonites, folds are easily overlooked and their importance may be underestimated. Is stretching parallel to the lineation, accompanied by lateral flow? The xenolith study shows that the situation is more complex and neither a simple shear zone nor an expanding pluton can explain the observed features.

The zone of ductile deformation in southern California is a large tectonic structure and may be explained with a top-to-the-west displacement, with development of a lineation and asymmetric microstructural features as proposed by Simpson (1984). This is not inconsistent with the results from the xenolith study ($a < b$). However, the simple shear deformation was a minor contribution to the overall strain of Santa

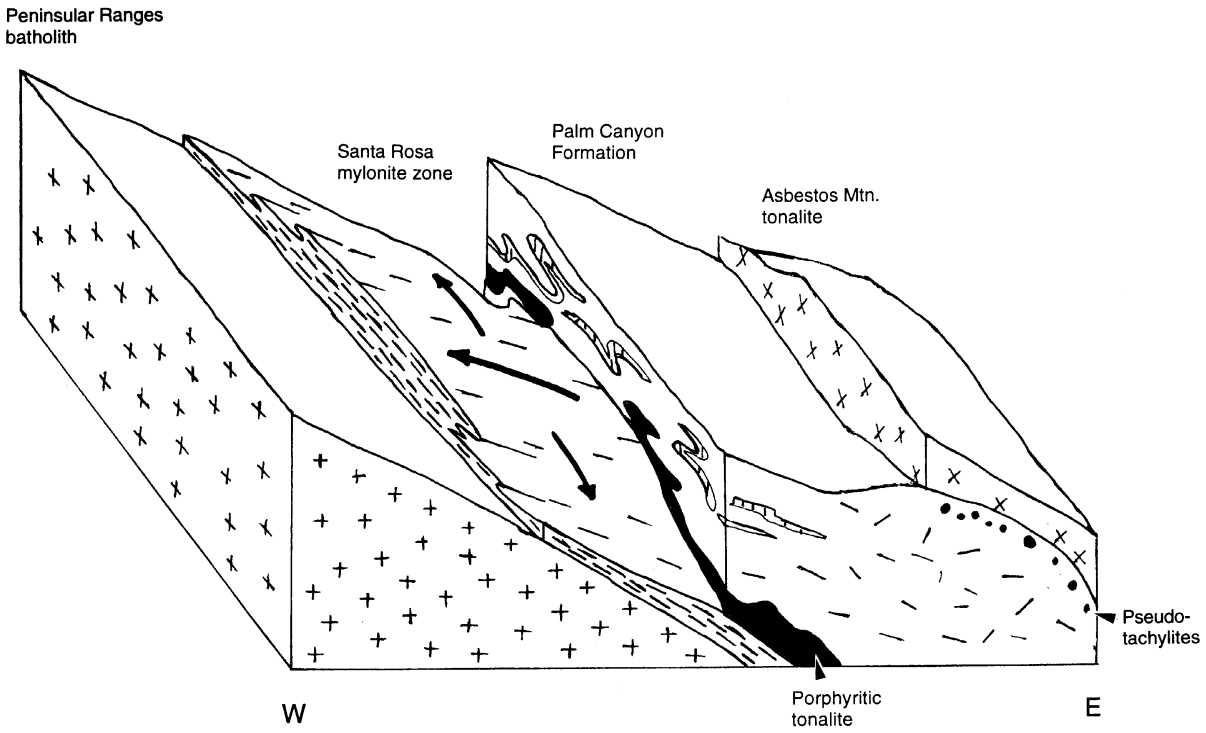

Fig. 14. Schematic block diagram illustrating the evolution of mylonites in Palm Canyon. A combination of top-to-the-southwest movement of the overlying Palm Canyon Formation and Asbestos Mountain tonalite and the emplacement of the Peninsular Ranges batholith with material flowing parallel to the lineation and simultaneous lateral spreading leads to folds and phyllonites.

Rosa mylonites (less than half) and may be expressed in the tendency for plane strain xenoliths in the southern zone (S3–S5). In the large and massive mylonite sequence in Palm Canyon most deformation occurred by flattening, and this may well be related to the emplacement of the partially solidified Peninsular ranges batholith, between Hermit's Bench and upper Palm Canyon. Deformation of the xenoliths may have started in a late igneous phase, but took place mainly in the solid state, associated with the development of a mylonitic foliation and lineation. The material deformed in a ductile manner, and quartz and mica have recrystallized. For these mylonites a hypothetical model is proposed in Fig. 14. The mylonitic and highly ductile rocks of Palm Canyon are squeezed between the overlying and more rigid metamorphic Palm Canyon–Asbestos Mtn. unit, with plenty of evidence for brittle deformation and high local stresses (e.g. a large pseudotachylite zone) and the emplacing Peninsular Ranges batholith. The material flow is consistent with the shear movement (top-to-the-southwest, e.g. the nappe-like emplacement of the Asbestos Mtn. tonalite) but also spreading laterally, resulting in local folding and thinning into phyllonites in which the lineation is much less defined. Within the wide spectrum of xenolith studies in plutonic rocks with different importance of magma emplacement and tectonic events, it appears that the case of the Santa Rosa mylonites is an example of the latter.

CONCLUSIONS

The study establishes that analysis of xenoliths is a relatively easy, quantitative and robust method to estimate large strain in granite mylonites and can be directly performed in the field. Xenoliths in Santa Rosa mylonites are highly flattened. But compared to diapiric intrusions, strains are an order of magnitude larger and xenoliths are elongated in the lineation direction. They represent an example of a complicated deformation process and can be used to determine the relative significance of large-scale tectonic processes and more local features, related to emplacement of cooling batholiths, in the formation of mylonites.

Acknowledgements—Constructive comments about the manuscript by J. Christie, K. McCaffrey and S. Treagus are greatly appreciated. I am indebted to many students and colleagues who accompanied me in Palm Canyon and discussed with me the many fascinating geological problems. Particularly useful were three summer field camps which I taught in this area. This study could not have been accomplished without having access to private roads, through courtesy of Michael Dunn (Palm Springs), the National Forest Service (Idyllwild) and the UC Deep Canyon Research Station. Jan Cecil contributed many stimulating ideas and helped with the preparation of the geological map. Support through NSF grant EAR-94-17580 is gratefully acknowledged.

REFERENCES

Ague, J. J. and Brimhall, G. H. (1988) Magmatic arc asymmetry and distribution of anomalous plutonic belts in the batholiths of

California: effects of assimilation, crustal thickness, and depth of crystallization. *Bulletin of the Geological Society of America* **100,** 912–927.

Balk, R. (1937) *The Structural Behavior of Igneous Rocks*. Memoirs of the Geological Society of America **5**.

Bateman, P. C. and Wahrhaftig, C. (1966) Geology of the Sierra Nevada. In *Geology of Northern California*, Bulletin 190, E. H. Bailey ed, pp. 107–172. Californian Division of Mines and Geology.

Cecil, J. D. (1990) A study of the Palm Canyon complex and related rocks, Riverside County, California. Unpublished Senior Thesis. University of California Berkeley.

Didier, J. and Barbarin, B. (1991) *Enclaves and Granite Petrology*. Elsevier, Amsterdam.

Dokka, R. K. (1984) Fission-track geochronological evidence for late Cretaceous mylonitization and early Paleocene uplift of the northeastern Peninsular Ranges, California. *Geophysical Research Letters* **11,** 46–49.

Erskine, B. C. and Wenk, H. -R. (1985) Evidence for late Cretaceous crustal thinning in the Santa Rosa mylonite zone, southern California. *Geology* **13,** 274–277.

Flinn, D. (1962) On folding during three-dimensional progressive deformation. *Quarterly Journal of the Geological Society of London* **118,** 385–433.

Goodwin, L. B. and Renne, P. R. (1991) Effects of progressive mylonitization on Ar retention in biotites from the Santa Rosa Mylonite Zone, California, and thermochronologic implications. *Contribitions to Mineralogy and Petrology* **108,** 283–297.

Goodwin, L. B. and Wenk, H. -R. (1995) Development of phyllonite from granodiorite: Mechanisms of grain-size reduction in the Santa Rosa mylonite zone, California. *Journal of Structural Geology* **17,** 689–707.

Guglielmo, G. (1993) Magmatic strains and foliation triple points of the Merrimac plutons, northern Sierra Nevada, California: implications for pluton emplacement and timing of subduction. *Journal of Structural Geology* **15,** 177–189.

Hill, R. I. and Silver, L. T. (1980) Strontium isotopic variability in the pluton of San Jacinto Peak, southern California. *EOS Transactions of the American Geophysical Union* **61,** 411.

Holder, M. T. (1981) Some aspects of intrusion and ballooning: the Ardara pluton. *Journal of Structural Geology* **3,** 89–95.

Hutton, D. H. W. (1982) A method for the determination of the initial shapes of deformed xenoliths in granitoids. *Tectonophysics* **85,** T45–T50.

Lisle, R. J. (1985) Geological Strain Analysis. In *A Manual for the R_f/ϕ Technique*. Pergamon Press, Oxford.

O'Brien, D. K., Wenk, H.-R., Ratschbacher, L. and Zhendong, Y. (1987) Preferred orientation of phyllosilicates in phyllonites and ultramylonites. *Journal of Structural Geology* **9,** 719–730.

Paterson, S. R. and Fowler, T. K. (1993) Re-examining pluton emplacement processes. *Journal of Structural Geology* **15,** 191–206.

Paterson, S. R. (1988) Cannibal Creek granite: post-tectonic 'ballooning' pluton or pre-tectonic piercement diapir? *Journal of Geology* **96,** 730–736.

Ramsay, J. G. and Huber, M. I. (1983) Strain Analysis. In *The Techniques of Modern Structural Geology*, Vol. 1. Academic Press, London.

Ramsay, J. G. (1967) *Folding and Fracturing of Rocks*. McGraw Hill, New York.

Ramsay, J. G. (1981) Emplacement mechanics of the Chindamora Batholith, Zimbabwe. *Journal of Structural Geology* **3,** 93.

Ramsay, J. G. (1989) Emplacement kinematics of a granite diapir: The Chindamora batholith, Zimbabwe. *Journal of Structural Geology* **11,** 191–209.

Rogers, T. H. (1965) *Geologic Map of California* 1:250 000. *Santa Ana Sheet*. Californian Division Mines and Geology.

Sharp, R. V. (1967) San Jacinto fault zone of the Peninsular Ranges of southern California. *Geological Society of America Bulletin* **78,** 705–729.

Sharp, R. V. (1979) Some characteristics of the eastern Peninsular Ranges mylonite zone: analysis of actual fault zones in bedrock. In Proceedings of Conference VII. *U.S. Geological Survey Open-file Report* **79-1239** 258–267.

Simpson, C. and Schmid, S. M. (1983) An evaluation of criteria to deduce the sense of movement in sheared rocks. *Geological Society of America Bulletin*. **94,** 1281–1288.

Simpson, C. (1984) Borrego Springs-Santa Rosa mylonite zone: A late Cretaceous west-directed thrust in southern California. *Geology* **12,** 8–11.

Sintubin, M., Wenk, H. -R. and Phillips, D. S. (1995) Texture development in platy materials: comparison of Bi2223 aggregates with phyllosilicate fabrics. *Material Science and Engineering* **A202,** 157–171.

Tobisch, O. T., Renne, P. R. and Saleeby, J. B. (1993) Deformation resulting from regional extension during pluton ascent and emplacement, central Sierra Nevada, California. *Journal of Structural Geology* **15,** 609–628.

Treagus, S. H., Hudleston, P. J. and Lan, L. (1996) Non-ellipsoidal inclusions as geological strain markers and competence indicators. *Journal of Structural Geology* **18,** 1167–1172.

Tullis, J., Snoke, A. W. and Todd, V. R. (1982) Penrose Conference Report: significance and petrogenesis of mylonitic rocks. *Geology* **10,** 227–230.

Tullis, T. E. (1976) Experiments on the origin of slaty cleavage and schistosity. *Geological Society of America Bulletin* **87,** 745–753.

Wenk, H. -R. and Pannetier, J. (1990) Texture development in deformed granodiorites from the Santa Rosa mylonite zone, southern California. *Journal of Structural Geology* **12,** 177–184.

Wenk, H. -R. (1973) The structure of the Bergell Alps. *Eclogae Geological Helvetiae* **66,** 255–291.